Microstructure and mechanical properties of Al−Mg$_2$Si composite fabricated in-situ by vibrating cooling slope

Shaya SAFFARI, Farshad AKHLAGHI

School of Metallurgy and Materials Engineering,
College of Engineering, University of Tehran, P. O. Box 11155-4563, Tehran, Iran

Abstract: An innovative semisolid technique termed as vibrating cooling slope (VCS) has been applied to producing in-situ Al−25%Mg$_2$Si (mass fraction) composite. The molten Al−16.5Mg−9.4%Si (mass fraction) alloy with 100 °C superheat was poured on the surface of an inclined copper plate (set at 45° inclined angle) while it was vibrated at a frequency of 40 Hz and an amplitude of 400 μm. After travelling the length of 40 cm on the slope, the resultant semisolid alloy was cast into a steel mold. For the purpose of comparison, reference composite samples were made by gravity casting (GC) and conventionally still cooling slope casting (CS) methods using the same alloy under identical conditions. The samples were hot extruded at 500 °C. It was concluded that the size of Mg$_2$Si particles was decreased by about 50% and 70% for the CS and VCS produced samples respectively when compared to that of the GC produced sample. Despite of their higher porosity contents, both the as-cast and hot-extruded VCS processed samples exhibited higher hardness, shear yield stress (SYS) and ultimate shear strength (USS) values as compared with their GC produced counterparts. These results were attributed to the refined and modified microstructure obtained via this newly developed technique.
Key words: in-situ composite; Al−Mg$_2$Si alloy; semi-solid processing; vibrating cooling slope; microstructure; shear punch test

1 Introduction

Al−Mg$_2$Si composites, due to their proper cast-ability, light weight and good wear resistance, meet the demand of weight reduction and fuel saving for high-performance applications such as automotive and aerospace industries. These excellent properties are attributed to the presence of Mg$_2$Si reinforcing phase with a high melting temperature, low density, high hardness, low coefficient of thermal expansion (CTE) and reasonably high elastic modulus. Several processing routes such as gravity casting [1], centrifugal casting [2], mechanical stirring [3], cooling slope [4−6], strain induced melt activated (SIMA) [7] and electromagnetic separation [8] have been used to produce the in-situ Al−Mg$_2$Si composites. However, due to the presence of coarse primary Mg$_2$Si particles with sharp corners in their microstructure, the mechanical properties of such composites prepared by conventional casting routs were not satisfactory.

It has been reported that the addition of various alloying elements such as B, Cu, Mn, Cr, Li, Si, P and Ce [9−19] can modify the morphology of primary and eutectic Mg$_2$Si particles. Other efforts have been focused on the modification of these structures by using the semi-solid processing methods [3−7]. The heat treatment of Al−Mg$_2$Si composites can also be effective in improving their mechanical properties by homogenizing the microstructure, re-distributing the alloying elements, dissolving soluble phases and spheroidizing the eutectic particles [20,21]. It has been reported that superheating can also be regarded as a simple and effective method for the modification of the morphology of Mg$_2$Si particles [22−24]. It has also been reported that the Al−Mg$_2$Si composites prepared by rapid solidification and mechanical alloying techniques exhibited very fine Mg$_2$Si particles distributed uniformly in the fine-grained matrix alloys [25−27]. However, such techniques are too expensive and complex for mass production [28]. Therefore, to prepare the cost-effective in-situ Al−Mg$_2$Si composites, simple modified casting routes are preferable.

Cooling slope casting is a semi-solid processing route which benefits from a simpler technology as compared with other alternative techniques. In this

process, molten metal is poured on the top of an inclined cooling plate, causing its acceleration and shearing by gravity. Then, the resultant semi-solid slurry is poured into a mold where it is solidified. It is then subsequently re-heated at a temperature within the freezing range of the alloy to generate a globular structure [29−32]. It has also been documented that applying ultrasonic or mechanical vibration to a solidifying melt can lead to the formation of a fine, non-dendritic and globular structure [33−35]. However, these techniques are very time consuming. To overcome such shortcomings, a new process, termed as vibrating cooling slope (VCS), has been developed [36,37], in which the conventional cooling slope casting and vibration casting methods have been combined into an integrated one for refining and modification of structures. In the VCS technique, there is no need to reheat the samples or to provide a prolonging vibration as are necessary for those parent methods. Therefore, this technique eliminates capital cost expenditures, reduces the number of required steps and hence reduces the cost of castings with modified structures. Over the last few years, efforts have been made to produce various types of Al alloys and Al−SiC composites by this technique [38−44]. In the present study, the VCS method has been applied to refining the size and to modify the morphology of primary Mg_2Si particles in the in-situ Al−Mg_2Si casting composites.

2 Experimental

The vibrating cooling slope apparatus used in the present investigation consists of a cooling slope made of copper plate (1000 mm × 120 × 10 mm) mounted on a steel frame. This assembly was fixed on a steel plate mounted on a table via four springs. A steel shaft was attached to this plate via two ball bearings. This shaft could rotate by means of an electric motor (2.2 kW, 2840 r/min) via two pulleys and a belt. A steel hammer was attached to the shaft through a hole which was drilled on it at a centric position so that a vertical vibration during rotation could be generated. The vibration frequency could be altered by using different sized pulleys, resulting in different rotation speeds of the shaft. The cooling slope surface was coated by boron nitride (BN) and also it was preheated up to 150 °C by means of a gas torch. Figure 1 represents the schematic view of this apparatus.

About 5 kg of commercially pure Al was melted in a graphite crucible in an electric resistance furnace. Then, weighted amounts of Mg and Si were added to the melt at 750 °C. The amounts of Mg and Si were calculated by considering 10% and 7% mass loss for these elements, respectively. After 5 min holding, the melt was poured

into a steel die to prepare the starting material having the chemical composition as shown in Table 1.
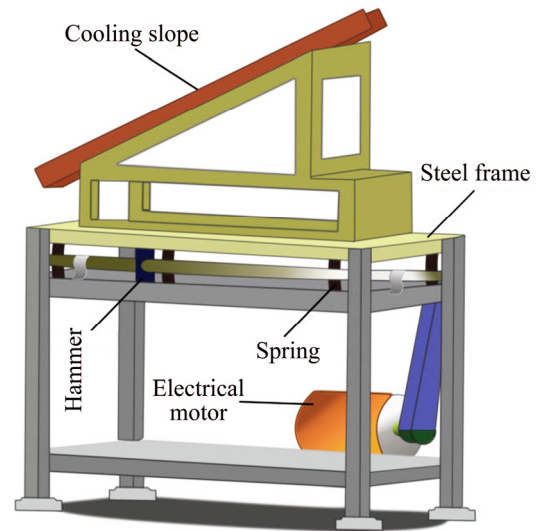

Fig. 1 Schematic representation of VCS apparatus

Table 1 Chemical composition of Al−Mg_2Si composite (mass fraction, %)

Mg	Si	Cr	Ni	Zn	Fe	Mn	Cu	Al
16.5	9.4	0.010	0.010	0.10	0.220	0.01	0.018	Bal.

For producing Al−25%Mg_2Si composite, this alloy was re-melted in a small graphite crucible (1 kg capacity) in a resistance furnace. The molten alloy at 880 °C (having 100 °C superheat) was poured on the surface of the slope plate (set at 45° inclined angle) while it was vibrated at a frequency of 40 Hz and an amplitude of 400 μm. The melt travelled the distance of 400 mm before being poured into a cylindrical cast-iron mold (60 mm in internal diameter and 34 mm in height). Also for the purpose of comparison, gravity casting (GC) as well as conventionally still cooling slope casting (CS) were carried out using the same mold and with the same superheat.

Extrusion was carried out via a hydraulic press at a ram speed of 1 mm/s while graphite based oil was used as the lubricant. Cylindrical bars with the length of 29 mm and diameter of 29 mm were cut and machined from the composite billets. These bars were homogenized at 520 °C for 4 h and furnace cooled to room temperature [45−47] and subsequently extruded at 500 °C with an extrusion ratio of 13:1.

Samples were sectioned from their geometrical center along their height and subjected to standard metallographic procedures. The microstructures of the specimens were examined using scanning electron microscope (SEM). The particle size and shape factor of the primary Mg_2Si particles were determined by an image analyzer using Clemex Vision Pro.Ver.3.5.025 software. For image processing, a total number of 100

randomly selected particles were analyzed in a total measured area of 300 mm^2 per specimen. The effective diameter (D_e) and shape factor (S_F) of the particles were calculated according to the following equations:

$$D_e = \sqrt{\frac{4A}{\pi}} \qquad (1)$$

$$S_F = \frac{4\pi A}{P^2} \qquad (2)$$

where P and A are the perimeter and surface area of the primary Mg$_2$Si particles, respectively. The standard deviation values obtained for each measurement were used for estimating the experimental errors.

The density values of the samples were quantified via the Archimedes' principle according to ISO 2738 standard using an electronic balance to an accuracy of 0.1 mg. Then, the porosity of each sample was calculated by considering its full density obtained via the rule-of-mixtures.

Hardness measurements were carried out on a Brinell hardness testing machine, using a load of 300 N, and the mean values of at least six measurements conducted on different areas of each sample were considered.

Shear punch test (SPT) was used to evaluate the strength values of composites [48−50]. This is an effective test method for evaluating mechanical properties such as the yield, ultimate strength, and strain hardening exponent values when the material availability is limited [49−56]. For composite materials, the small and simple specimen configurations required for SPT have advantages of reducing the costs and complexity associated with machining large standard tensile test samples. Several researchers have reported the correlations between the tensile and the SPT stresses [51,57−59].

Slices of the composite bars with 1 mm in thickness were wire-cut from both the as-machined and hot-extruded bars and were ground to a thickness of 0.8 mm, from which disks of 10 mm in diameter were punched for the SPT. Shear punch tests were carried out at room temperature using a cylindrical punch with 3.175 mm in diameter and with a flat end that penetrated into the material against a 3.225 mm diameter receiving die at a constant cross-head speed of 0.25 mm/min. The schematic view of this shear punch-die assembly is shown in Fig. 2.

The variation in punching load with the ram displacement was continuously recorded and the obtained data set was used for determination of the shear stress, τ, using the following relationship:

$$\tau = \frac{P_1}{\pi dt} \qquad (3)$$

where P_1 is the punch load, t is the specimen thickness and d is the average diameter of the punch and die. The reproducibility of this testing technique was confirmed by obtaining nearly the same results from testing three different samples prepared under an identical condition.
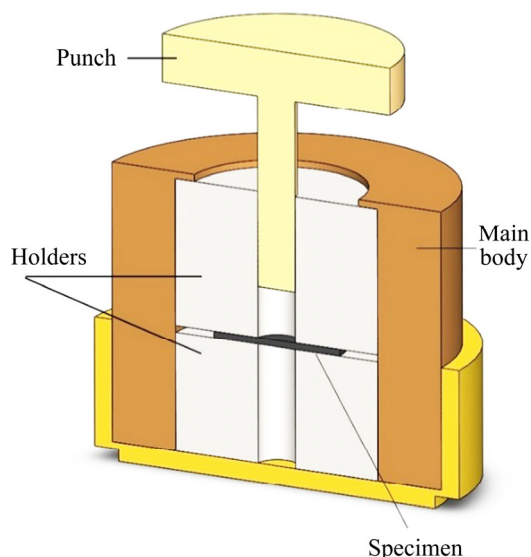

Fig. 2 Schematic representation of shear punch−die assembly

3 Results and discussion

Figures 3(a)−(c) represent the as-cast microstructures of Al−25%Mg$_2$Si composites prepared by GC, CS, and VCS methods, respectively. According to Fig. 3(a), the gravity casting resulted in the formation of coarse primary Mg$_2$Si particles surrounded by α(Al) in the Al/Mg$_2$Si eutectic matrix. The morphology of the primary unmodified Mg$_2$Si particles in this sample is irregular and dendritic. Similar dendritic morphology of primary Mg$_2$Si in unmodified Al−Mg$_2$Si composites has also been reported in the previous investigations [1−20].

A comparison between Figs. 3(a) and (b) reveals the significant decrease in the Mg$_2$Si particle size in the CS produced composite as compared with the GC produced composite. It can also be seen that the morphology of the Mg$_2$Si particles has been changed from dendritic in the GC to polyhedral in the CS specimen. Figure 3(c) shows that the VCS process resulted in considerably finer and more spherically shaped primary Mg$_2$Si particulates as compared with the CS process.

The effective diameter (D_e) and the shape factor (S_F) of the primary Mg$_2$Si particles in the specimens prepared by these three different routes are listed in Table 2. These data also confirm the refinement of Mg$_2$Si particles (about 50%) in the CS processed sample as compared with GC process. It can be seen that, as compared with GC process, when the cooling slope was vibrated during the process, about 70% reduction in the size of the Mg$_2$Si
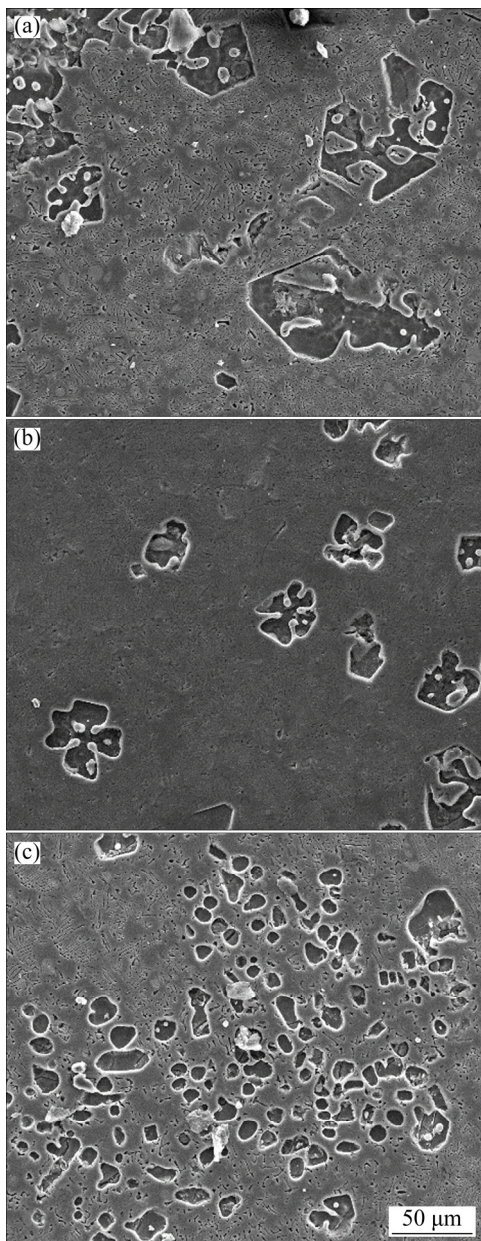
Fig. 3 Typical SEM micrographs of as-cast Al−25%Mg$_2$Si composites prepared by GC (a), CS (b) and VCS (c) methods

Table 2 Effective diameter (D_e) and shape factor (S_F) of primary Mg$_2$Si particles generated by different casting routes

Casting route	D_e/μm	S_F
Gravity casting(GC)	121.5±23.04	0.54±0.18
Still cooling slope(CS)	63.7±17.29	0.66±0.12
Vibrating cooling slope(VCS)	33.8±8.75	0.7±0.14

particles was obtained. According to Table 2, using the CS method resulted in increased shape factor (sphericity) of the Mg$_2$Si particles as compared with the GC method. The shape factor of particles in the VCS processed

sample was larger than that of the CS processed sample. However, by considering the experimental errors presented in this Table, the shape factor values obtained in these three different processed samples are close to each other. In other words, insignificant improvement in the shape factor of the Mg$_2$Si particles can be obtained when CS and/or VCS techniques are used instead of the conventional casting.

The refined size of the primary Mg$_2$Si particles generated by conventional cooling slope can be attributed to the multiple nucleation of this phase during the flow of molten metal on the surface of the copper plate. A number of these nuclei are detached from the surface as a result of applying shear stress and are distributed into the melt to generate a large number of refined primary Mg$_2$Si particles. The decreased size of the Mg$_2$Si particles in the VCS processed sample as compared with that of the CS specimen can be explained as follows: during the flow of molten metal on the VCS, lots of nuclei are formed on the cooling slope. These nuclei are subsequently detached from the surface due to the combined effects of shearing on the cooling slope and application of vertical vibration. The vibration intensifies the detachment of the generated nuclei from the surface and provides increased number of nuclei. Therefore, the volume fraction of nuclei suspended in the molten alloy entering the mold cavity is increased and consequently the size of the Mg$_2$Si particles is decreased.

In addition, the vibration of cooling slope suppresses the denderitic growth by fragmentation of the growing dendrites by several mechanisms such as: 1) intensified flow of the liquid metal around dendrite arms; 2) bending stresses induced on the growing dendrites due to the vibration induced movement of the liquid between them and 3) re-melting of dendrite arms at the necks due to the increased temperature fluctuation as a consequence of strong motion of liquid [35,60,61]. In the VCS technique, the formation and fragmentation of the dendrite arms may occur in the partially solidified flowing melt near the contact surface of the cooling slope. Based on these mechanisms, the crystals formed by detachment of the weak dendrite arms along the cooling plate grow in the mold. In the present work, vibration of the slope resulted in much pronounced fragmentation of dendrite arms and intensified detachment of them from the cooling plate. These events provide more sites for heterogeneous nucleation of new crystals. The number of the seed crystals and the extent of the shear stress applied on them are therefore affected by the vibration action. Consequently, the applied vibration increases the number of nucleated crystals and intensifies their fragmentation process, resulting in the decreased size of the Mg$_2$Si particles. Also both the flow

of the molten metal on the cooling slope and vibration in the solidifying melt contribute to the increased shear stress applied on the growing crystals and result in the generation of more spherical particles as compared to gravity casting. It is interesting to note that the inspection of the cooling plate after our conventional cooling slope experiments revealed the formation of a solidified alloy skin on the surface of the copper plate. This skin was formed by the growth of those primary nuclei that adhered to the plate and ended up with a layer of solidified alloy. This layer retarded the effectiveness of the plate in generating nuclei. However, we could not detect any solidified skin on the surface of the copper plate at the conclusion of the VCS process. In this case, the nuclei could not remain on the plate and therefore the formation of the solidified skin was inhibited. This can be regarded as another reason for obtaining finer Mg_2Si particles in the VCS method as compared with conventional CS technique.

The microstructures of hot-extruded Al−25%Mg_2Si composites prepared by three different methods of GC, CS, and VCS methods are shown in Figs. 4(a)−(c), respectively. A comparison between this figure and Fig. 3 reveals that during hot extrusion the morphology of the Mg_2Si particles was not changed considerably. However, the hot extrusion process may have resulted in the breakup of a part of the reinforcing hard Mg_2Si particles and imposing a non-uniform distribution of different sized particles in the matrix. A comparison between Figs. 3(c) and 4(c) confirms this postulation.

The porosities of Al−25%Mg_2Si composites prepared by three different casting routes in the as-cast and hot-extruded conditions are compared to each other in Fig. 5. The increased porosity of the as-cast CS processed sample as compared with that of the GC produced sample is attributed to: 1) a high turbulence induced to the melt during its flow on the slope and 2) the increased viscosity of the slurry entering the mould cavity that retards the escape of the entrapped gas bubbles from the melt before solidification. Both the above mentioned mechanisms are intensified during vibration of the cooling slope, resulting in the increased porosity of the VCS sample. It can be seen that hot extrusion process reduced the porosity of these three different samples effectively.

However, complete removal of porosities did not occur. It is important to note that the extrusion process only eliminates those pores which are smaller than a critical size. In other words, larger pores only become smaller during hot-extrusion process at a certain extrusion ratio. Therefore, for gaining full densification by applying extrusion process, it is required to decrease the critical size of pores by increasing the extrusion ratio [62].
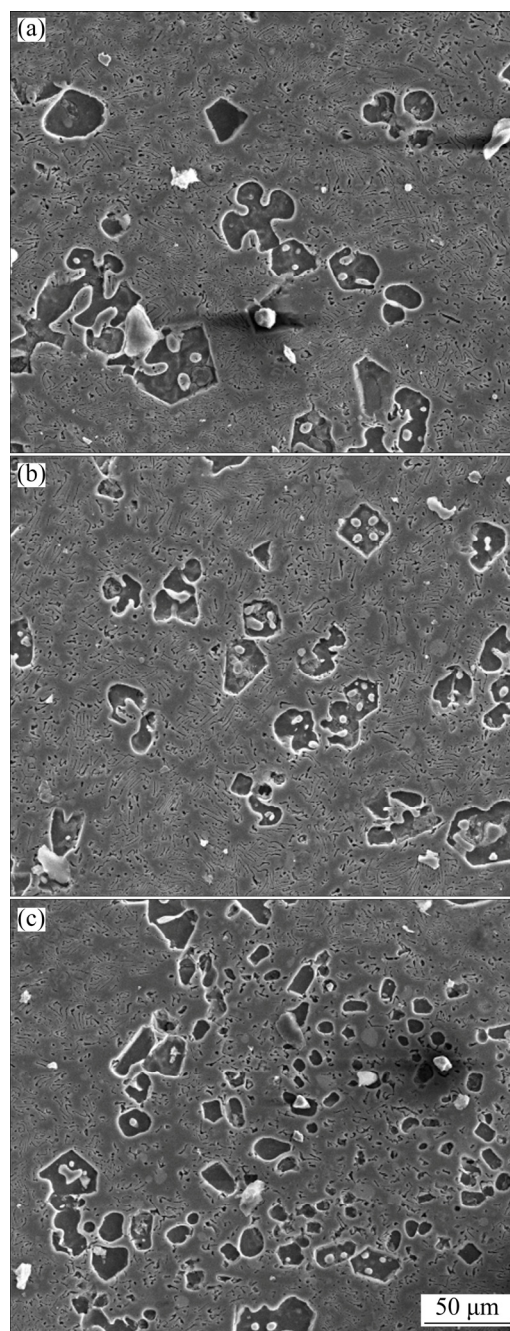

Fig. 4 Typical SEM micrographs of hot-extruded Al−25%Mg_2Si composites prepared by GC (a), CS (b) and VCS (c) methods (The extrusion direction is perpendicular to the shown micrographs)

Figure 6 shows the hardness values of the Al−25%Mg_2Si composites generated by three different casting routes in the as-cast and hot-extruded conditions. It can be seen that for the as-cast composites, the CS processed sample exhibits a higher hardness as compared with GC produced sample.

Also an insignificant increase in the hardness of the sample can be observed when vibration was applied on the cooling slope. These results can be attributed to the decreased size and increased shape factor of Mg_2Si
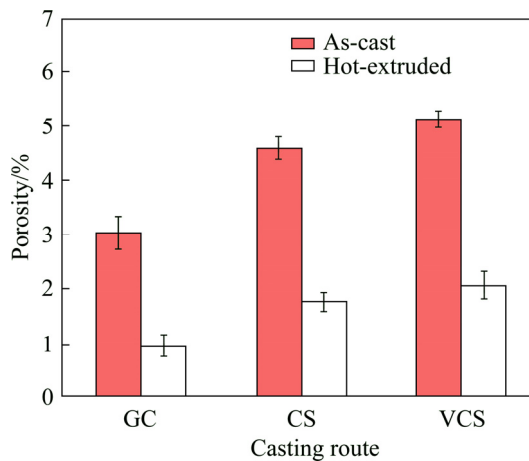
Fig. 5 Porosities of Al−25%Mg$_2$Si composites prepared by different casting routes in as-cast and hot-extruded conditions
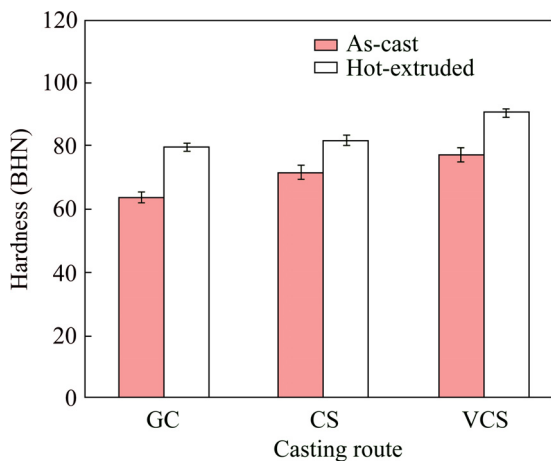

Fig. 6 Hardness of Al−25%Mg$_2$Si composites prepared by different casting routes in as-cast and hot-extruded conditions

particles by using CS or VCS methods instead of GC method (Table 2). However, it is obvious that the presence of pores results in decreased hardness of samples. According to Fig. 5, The CS and VCS samples are more porous than the GC processed one; therefore, a part of the beneficial effect of the refined and modified Mg$_2$Si particles in the CS and VCS samples is diminished due to their higher porosity. The increased hardness of the hot-extruded samples as compared with their as-cast counterparts is attributed to their lower porosity levels (as shown in Fig. 5) as well as the decreased size of their Mg$_2$Si particles.

The shear deformation behavior of the composites prepared by three different casting routes in both the as-cast and hot extruded conditions was investigated by shear punch test. This technique has proved to be capable of providing strength data, which are well correlated with the conventional tensile test data [56,63]. For each sample, the measured room temperature punching load was converted to shear stress by using Eq. (3), and the results were plotted against the normalized displacement,

as shown in Figs. 7(a) and (b). It can be observed that each of the individual curves exhibits a linear part, followed by a deviation from linearity. Further loading of the specimens results in the load instability, at which a maximum is observed in the stress−displacement curves. The deviation point is taken as the shear yield stress (SYS), and the stress corresponding to the maximum point is referred to as the ultimate shear strength (USS) [64]. The resultant SYS and USS values for different samples are presented in Figs. 8(a) and (b), respectively. It can be seen that the VCS samples exhibit the highest SYS and USS values, while the GC samples demonstrate the lowest values for those properties. The SYS and USS values of the CS samples are between the GC and VCS specimens. Figure 8 reveals that despite of their higher porosity levels (Fig. 5), the as-cast CS and VCS samples exhibit improved mechanical properties as compared with the GC processed composite.

These results can be attributed to the beneficial effects of the modified and refined Mg$_2$Si particles (Fig. 3 and Table 2) on improving the mechanical properties of the composites that overweighed the
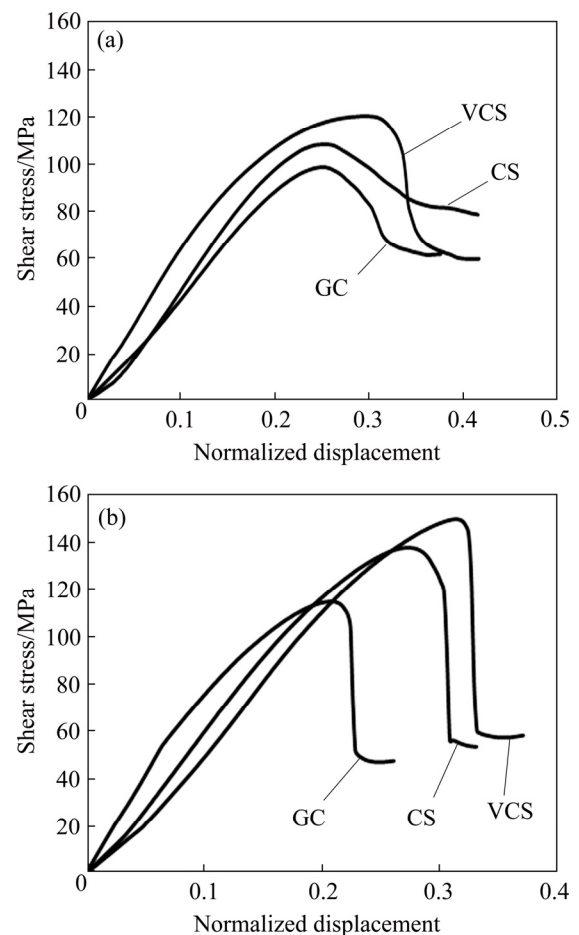

Fig. 7 Shear stress−normalized displacement curves of as-cast (a) and hot-extruded (b) composites prepared by three different routes
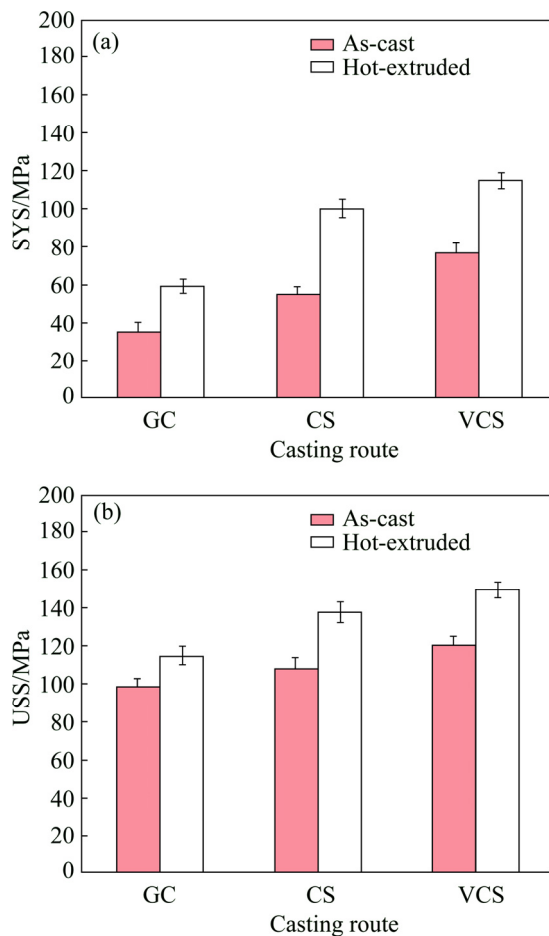
Fig. 8 Values of SYS (a) and USS (b) of Al−25%Mg$_2$Si composites prepared by three different casting routes in as-cast and hot-extruded conditions

detrimental effects of increased porosity. According to Fig. 8, the SYS and USS of all the as-cast composites are improved by hot-extrusion process. These results are attributed to the decreasing porosity levels (Fig. 5) as well as refining the microstructure of the as-cast composites during hot-extrusion which is evident by comparing Figs. 3 and 4.

4 Conclusions

1) The application of the cooling slope (CS) technique for processing of in-situ Al−Mg$_2$Si composites results in a considerable decrease in the size of Mg$_2$Si particles accompanied with a slight increase in their shape factor as compared with gravity casting (GC) method. These effects are intensified when vibration is applied on the cooling slope in the vibrating cooling slope (VCS) method.

2) Despite of the higher porosity of the as-cast VCS and CS processed samples as compared with that of the GC specimen, the former ones exhibit higher hardness, shear yield stress (SYS) and ultimate shear strength

(USS) values attributable to their refined and modified microstructures. The hardness, SYS and USS values of the as-cast VCS sample are higher than those of its CS counterpart due to its finer microstructure.

3) Hot extrusion results in increased hardness and improved mechanical properties (i.e., increased SYS and USS values) of all the Al−Mg$_2$Si composites processed via the three investigated casting routes. These results are attributed to the decreased porosity as well as the refinement of both the primary and eutectic Mg$_2$Si particles during the hot extrusion process. The hardness, SYS and USS of the hot-extruded VCS processed Al−Mg$_2$Si composite are BHN 95, 120 MPa and 140 MPa, respectively, being higher than those of all the other investigated samples.

References

[1] LI C, WU Y, LI H, LIU X. Morphological evolution and growth mechanism of primary Mg$_2$Si phase in Al−Mg$_2$Si alloys [J]. Acta Materialia, 2011, 59(3): 1058−1067.

[2] ZHANG J, FAN Z, WANG Y, ZHOU B. Hypereutectic aluminium alloy tubes with graded distribution of Mg$_2$Si particles prepared by centrifugal casting [J]. Materials & Design, 2000, 21(3): 149−153.

[3] ATKINSON H V. Modelling the semisolid processing of metallic alloys [J]. Progress in Materials Science, 2005, 50(3): 341−412.

[4] QIN Q, ZHAO Y, CONG P, ZHOU W, XU B. Semisolid microstructure of Mg$_2$Si/Al composite by cooling slope cast and its evolution during partial remelting process [J]. Materials Science and Engineering A, 2007, 444(1): 99−103.

[5] SAGHAFIAN H, SHABESTARI S, GHONCHEH M, SAHIHI F. Wear behavior of thixoformed Al−25wt.%Mg$_2$Si composites produced by slope casting method [J]. Tribology Transactions, 2015, 58(2): 288−299.

[6] SHABESTARI S, SAGHAFIAN H, SAHIHI F, GHONCHEH M. Investigation on microstructure of Al−25wt%Mg$_2$Si composite produced by slope casting and semi-solid forming [J]. International Journal of Cast Metals Research, 2015, 28(3): 158−166.

[7] QIN Q, ZHAO Y, XIU K, ZHOU W, LIANG Y. Microstructure evolution of in situ Mg$_2$Si/Al−Si−Cu composite in semisolid remelting processing [J]. Materials Science and Engineering A, 2005, 407(1): 196−200.

[8] SONG C J, XU Z M, LIANG G, LI J G. Study of in-situ Al/Mg$_2$Si functionally graded materials by electromagnetic separation method [J]. Materials Science and Engineering A, 2006, 424(1): 6−16.

[9] AZARBARMAS M, EMAMY M, ALIPOUR M, RASSIZADEHGHANI J. The effects of boron additions on the microstructure, hardness and tensile properties of in situ Al−15% Mg$_2$Si composite [J]. Materials & Design, 2011, 32(10): 5049−5054.

[10] EMAMY M, NEMATI N, HEIDARZADEH A. The influence of Cu-rich intermetallic phases on the microstructure, hardness and tensile properties of Al−15%Mg$_2$Si composite [J]. Materials Science and Engineering A, 2010, 527(12): 2998−3004.

[11] GHORBANI M, EMAMY M, KHORSHIDI R, RASIZA-DEHGHANI J, EMAMY A. Effect of Mn addition on the microstructure and tensile properties of Al−15% Mg$_2$Si composite [J]. Materials Science and Engineering A, 2012, 550(1): 191−198.

[12] GHORBANI M, EMAMY M, NEMATI N. Microstructural and mechanical characterization of Al−15%Mg$_2$Si composite containing chromium [J]. Materials & Design, 2011, 32(8): 4262−4269.

[13] HADIAN R, EMAMY M, VARAHRAM N, NEMATI N. The effect of Li on the tensile properties of cast Al−Mg$_2$Si metal matrix composite [J]. Materials Science and Engineering A, 2008, 490(1): 250−257.

[14] LI C, WU Y, LI H, LIU X. Microstructural formation in hypereutectic Al−Mg$_2$Si with extra Si [J]. Journal of Alloys and Compounds, 2009, 477(1): 212−216.

[15] NORDIN N A, FARAHANI S, ABUBAKR T, HAMZAH E. Alteration by cerium element on primary and eutectic Mg$_2$Si phases in Al−20%Mg$_2$Si in situ composite [J]. Advanced Materials Research, 2015, 1125: 23−27.

[16] QIN Q, ZHAO Y, ZHOU W, CONG P. Effect of phosphorus on microstructure and growth manner of primary Mg$_2$Si crystal in Mg$_2$Si/Al composite [J]. Materials Science and Engineering A, 2007, 447(1): 186−191.

[17] ZHANG J, FAN Z, WANG Y, ZHOU B. Microstructural development of Al−15wt.%Mg$_2$Si in situ composite with mischmetal addition [J]. Materials Science and Engineering A, 2000, 281(1): 104−112.

[18] ZHANG J, FAN Z, WANG Y, ZHOU B. Microstructural evolution of the in situ Al−15wt.%Mg$_2$Si composite with extra Si contents [J]. Scripta Materialia, 2000, 42(11): 1101−1106.

[19] ZHAO Y, QIN Q, ZHOU W, LIANG Y. Microstructure of the Ce-modified in situ Mg$_2$Si/Al−Si−Cu composite [J]. Journal of Alloys and Compounds, 2005, 389(1): L1−L4.

[20] MALEKAN A, EMAMY M, RASSIZADEHGHANI J, EMAMY A. The effect of solution temperature on the microstructure and tensile properties of Al−15%Mg$_2$Si composite [J]. Materials & Design, 2011, 32(5): 2701−2709.

[21] SJÖLANDER E, SEIFEDDINE S. The heat treatment of Al−Si−Cu−Mg casting alloys [J]. Journal of Materials Processing Technology, 2010, 210(10): 1249−1259.

[22] MIN Z, WANG H Y, BO L, BING Z, LIANG M I, DONG L, JIANG Q C. Influence of melt superheating on microstructures of Mg−3.5Si−1Al alloys [J]. Transactions of Nonferrous Metals Society of China, 2008, 18: 107−112.

[23] QIN Q, ZHAO Y, LIANG Y, ZHOU W. Effects of melt superheating treatment on microstructure of Mg$_2$Si/Al−Si−Cu composite [J]. Journal of Alloys and Compounds, 2005, 399(1): 106−109.

[24] SAFFARI S, AKHLAGHI F. Influence of melt superheating on microstructure evolution in Al−Mg$_2$Si composites fabricated by gravity casting and vibrating cooling slope methods [C]//Proc Iran International Aluminum Conference (IIAC2014). Tehran, Iran, 2014: 14.

[25] FROMMEYER G, BEER S, von OLDENBURG K. Microstructure and mechanical properties of mechanically alloyed intermetallic Mg$_2$Si−Al alloys [J]. Zeitschrift für Metallkunde, 1994, 85(5): 372−377.

[26] MABUCHI M, HIGASHI K. Strengthening mechanisms of Mg$_2$Si alloys [J]. Acta Materialia, 1996, 44(11): 4611−4618.

[27] QIN Q, ZHAO Y. Nonfaceted growth of intermetallic Mg$_2$Si in Al melt during rapid solidification [J]. Journal of Alloys and Compounds, 2008, 462(1): L28−L31.

[28] MOSLEH-SHIRAZI S, AKHLAGHI F. Effect of SiC content on dry sliding wear, corrosion and corrosive wear of Al/SiC nanocomposites [J]. Transactions of Nonferrous Metals Society of China, 2016, 26: 1801−1808.

[29] PILLAI R, KUMAR K B, PAI B. A simple inexpensive technique for enhancing density and mechanical properties of Al−Si alloys [J]. Journal of Aaterials Processing Technology, 2004, 146(3): 338−348.

[30] KUND N K, DUTTA P. Numerical simulation of solidification of liquid aluminum alloy flowing on cooling slope [J]. Transactions of Nonferrous Metals Society of China, 2010, 20(S): s898−s905.

[31] KHOSRAVI H, ESLAMI-FARSANI R, ASKARI-PAYKANI M. Modeling and optimization of cooling slope process parameters for semi-solid casting of A356 Al alloy [J]. Transactions of Nonferrous Metals Society of China, 2014, 24: 961−968.

[32] HAGA T, NAKAMURA R, TAGO R, WATARI H. Effects of casting factors of cooling slope on semisolid condition [J]. Transactions of Nonferrous Metals Society of China, 2010, 20(S): s968−s972.

[33] TSUNEKAWA Y, SUZUKI H, GENMA Y. Application of ultrasonic vibration to in situ MMC process by electromagnetic melt stirring [J]. Materials & Design, 2001, 22(6): 467−472.

[34] SARAJAN Z. Ultrasonic modification of A356−Al$_2$O$_3$ composites [J]. Metallurgical Research & Technology, 2016, 113(2): 202−212.

[35] ZHAO J W, WU S S, XIE L Z, PING A, MAO Y W. Effects of vibration and grain refiner on microstructure of semisolid slurry of hypoeutectic Al−Si alloy [J]. Transactions of Nonferrous Metals Society of China, 2008, 18: 842−846.

[36] GUAN R G, WANG C, XING Z H, LEE C S, HU F Y. Novel slope plate process for semisolid forming [J]. Materials Science and Technology, 2007, 23(4): 438−443.

[37] GUAN R G, ZHANG L, WANG C, WEN J, CUI J. Three-dimensional analysis of the modified sloping/cooling/shearing process [J]. J Univ Sci Technol Beiging: Mineral Metall Mater, 2007, 14(2): 146−150.

[38] AKHLAGHI F, TAGHANI A. Development of vibrating cooling slope (VCS) method for enhancing a globular structure in aluminum A356 alloy [C]//Proc 12th International Conference on Aluminum Alloys. Yokohama, Japan, 2010: 1839−1844.

[39] GUAN R G, ZHAO Z Y, LI Y D, CHEN T J, XU S X, QI P X. Microstructure and properties of squeezing cast A356 alloy processed with a vibrating slope [J]. Journal of Materials Processing Technology, 2016, 229: 514−519.

[40] GUAN R G, ZHAO Z Y, CHAO R Z, ZHAO H L, LIU C M. Effects of technical parameters of continuous semisolid rolling on microstructure and mechanical properties of Mg−3Sn−1Mn aloy [J]. Transactions of Nonferrous Metals Society of China, 2013, 23: 73−79.

[41] GUAN R G, ZHAO Z Y, CHAO R Z, FENG Z X, LIU C M. Microstructure evolution and solidification behaviors of A2017 alloy during cooling/stirring and rolling process [J]. Transactions of Nonferrous Metals Society of China, 2012, 22: 2871−2876.

[42] GUAN R G, CAO F, CHEN L, LI J, WANG C. Dynamical solidification behaviors and microstructural evolution during vibrating wavelike sloping plate process [J]. Journal of Materials Processing Technology, 2009, 209(5): 2592−2601.

[43] GENCALP S, SAKLAKOGLU N. Semisolid microstructure evolution during cooling slope casting under vibration of A380 aluminum alloy [J]. Materials and Manufacturing Processes, 2010, 25(9): 943−947.

[44] KHOSRAVI H, AKHLAGHI F. Comparison of microstructure and wear resistance of A356−SiC$_p$ composites processed via compocasting and vibrating cooling slope [J]. Transactions of Nonferrous Metals Society of China, 2015, 25: 2490−2498.

[45] BAHRAMI A, RAZAGHIAN A, EMAMY M, KHORSHIDI R. The effect of Zr on the microstructure and tensile properties of hot-extruded Al−Mg$_2$Si composite [J]. Materials & Design, 2012, 36: 323−330.

[46] EMAMY M, YEGANEH S V, RAZAGHIAN A, TAVIGHI K. Microstructures and tensile properties of hot-extruded Al matrix composites containing different amounts of Mg$_2$Si [J]. Materials Science and Engineering A, 2013, 586: 190−196.

[47] RAZAGHIAN A, BAHRAMI A, EMAMY M. The influence of Li on the tensile properties of extruded in situ Al−15% Mg$_2$Si composite [J]. Materials Science and Engineering A, 2012, 532: 346−353.

[48] ALIZADEH R, MAHMUDI R, NGAN A, HUANG Y, LANGDON T. Superplasticity of a nano-grained Mg−Gd−Y−Zr alloy processed by high-pressure torsion [J]. Materials Science and Engineering A, 2016, 651: 786−794.

[49] GOLMAKANIYOON S, MAHMUDI R. Effect of aging treatment on the microstructure, creep resistance and high-temperature mechanical properties of Mg−6Zn−3Cu alloy with La-and Ce-rich rare earth additions [J]. Materials Science and Engineering A, 2015, 620: 301−308.

[50] SAFARI A, MAHMUDI R. High temperature mechanical properties of an extruded Mg−TiO₂ nano−composite [J]. Advanced Engineering Materials, 2015, 17(11): 1639−1644.

[51] GUDURU R, DARLING K, KISHORE R, SCATTERGOOD R, KOCH C, MURTY K. Evaluation of mechanical properties using shear–punch testing [J]. Materials Science and Engineering A, 2005, 395: 307−314.

[52] LEON C, DREW R. Small punch testing for assessing the tensile strength of gradient Al/Ni−SiC composites [J]. Materials Letters, 2002, 56(5): 812−816.

[53] ZHANG L, ELWAZRI A, ZIMMERLY T, BROCHU M. Shear punch testing and fracture toughness of bulk nanostructured silver [J]. Materials & Design, 2009, 30(5): 1445−1450.

[54] KURTZ S, JEWETT C, BERGSTRÖM J, FOULDS J, EDIDIN A. Miniature specimen shear punch test for UHMWPE used in total joint replacements [J]. Biomaterials, 2002, 23(9): 1907−1919.

[55] ALIZADEH R, MAHMUDI R. Evaluating high-temperature mechanical behavior of cast Mg−4Zn−xSb magnesium alloys by shear punch testing [J]. Materials Science and Engineering A, 2010, 527: 3975−3983.

[56] GUDURU R K, NAGASEKHAR A V, SCATTERGOOD R O, KOCH C C, MURTY K L. Thickness and clearance effects in shear punch testing [J]. Advanced Engineering Materials, 2007, 9(3): 157−160.

[57] TOLOCZKO M, HAMILTON M, LUCAS G. Ductility correlations between shear punch and uniaxial tensile test data [J]. Journal of Nuclear Materials, 2000, 283: 987−991.

[58] HANKIN G, TOLOCZKO M, HAMILTON M, FAULKNER R. Validation of the shear punch–tensile correlation technique using irradiated materials [J]. Journal of Nuclear Materials, 1998, 258: 1651−1656.

[59] HAMILTON M, TOLOCZKO M. Effect of low temperature irradiation on the mechanical properties of ternary V−Cr−Ti alloys as determined by tensile tests and shear punch tests [J]. Journal of Nuclear Materials, 2000, 283: 488−491.

[60] KOCATEPE K, BURDETT C. Effect of low frequency vibration on macro and micro structures of LM6 alloys [J]. Journal of Materials Science, 2000, 35(13): 3327−3335.

[61] ZHANG J, FAN Z, WANG Y, ZHOU B. Effect of cooling rate on the microstructure of hypereutectic Al−Mg₂Si alloys [J]. Journal of Materials Science Letters, 2000, 19(20): 1825−1828.

[62] TEKMEN C, OZDEMIR I, COCEN U, ONEL K. The mechanical response of Al−Si−Mg/SiCₚ composite: influence of porosity [J]. Materials Science and Engineering A, 2003, 360(1): 365−371.

[63] MASOUDPANAH S, MAHMUDI R. The microstructure, tensile, and shear deformation behavior of an AZ31 magnesium alloy after extrusion and equal channel angular pressing [J]. Materials & Design, 2010, 31(7): 3512−3517.

[64] ALIZADEH R, MAHMUDI R. Microstructural characterization and high−temperature mechanical behavior of cast Mg−4Zn−xSi alloys [J]. Advanced Engineering Materials, 2014, 16(9): 1160−1166.

振动斜板冷却法制备原位 Al−Mg₂Si 复合材料的显微组织和力学性能

Shaya SAFFARI, Farshad AKHLAGHI

School of Metallurgy and Materials Engineering,
College of Engineering, University of Tehran, P. O. Box 11155-4563, Tehran, Iran

摘　要：采用被称为振动斜板冷却法(VCS)的一种新型半固态成型技术制备 Al−25%Mg₂Si 原位复合材料。将熔化的 Al−16.5%Mg−9.4%Si 合金(过热 100 °C)浇铸到振动的倾斜铜板表面(倾斜角为 45°)，其振动频率为 40 Hz，振幅为 400 μm。在斜板上移动 40 cm 后，将合成的半固态合金铸入钢模中。为了对比，采用重力铸造法(GC)和传统的静止斜板冷却浇铸法(CS)制备合金成分相同的复合材料。将复合材料样品在 500 °C 进行热挤压。与 GS 制备的合金相比，采用 CS 和 VCS 制备的合金中 Mg₂Si 颗粒尺寸分别减小了 50%和 70%。与 GC 制备的样品相比，VCS 制备的浇铸态和热挤压态样品，尽管其孔隙率较大，但具有更高的硬度、剪切屈服应力(SYS)和剪切极限强度(USS)，这是由于通过这种新型的 VCS 方法可以得到更细小的微观组织。

关键词：原位复合材料；Al−Mg₂Si 合金；半固态加工；振动斜板冷却；显微组织；剪切冲孔试验

(Edited by Wei-ping CHEN)